Desalination and Water Treatment
www.deswater.com
doi: 10.5004/dwt.2022.28292

253 (2022) 63–77
March

Impact of municipal wastewater and sulfur springs on the physicochemical properties of the Euphrates River, Western Iraq

Muwafaq Ayesh Rabeea[a,*], Tahseen A. Zaidan[a], Ahmed J.R. Al-Heety[b], Ahmed S. Al-Rawi[c], Mohamed Elhag[d,e,f,g,*]

[a]*Department of Applied Chemistry, College of Applied Sciences, University Of Anbar, Hit, Anbar 31007, Iraq, email: muw88@uoanbar.edu.iq (M.A. Rabeea)*
[b]*Seismic Processing Center, Oil Exploration Company, Baghdad, Iraq*
[c]*Department of Chemistry, College of Sciences, University Of Anbar, Anbar, Iraq*
[d]*Department of Hydrology and Water Resources Management, Faculty of Meteorology, Environment and Arid Land Agriculture, King Abdulaziz University, Jeddah 21589, Saudi Arabia, email: melhag@kau.edu.sa*
[e]*Institute of Remote Sensing and Digital Earth (RADI), Chinese Academy of Science (CAS), Beijing 100094, China*
[f]*Department of Applied Geosciences, Faculty of Science, German University of Technology in Oman, Muscat 1816, Oman*
[g]*Department of Geoinformation in Environmental Management, CI-HEAM/Mediterranean Agronomic Institute of Chania, Chania 73100, Greece*

Received 8 September 2021; Accepted 10 February 2022

ABSTRACT

In this study, the environmental damage of Euphrates water caused by the three main sources of wastewater (municipal wastewater and tar spring water) in the Hit sector was investigated. Surface water monitoring was performed by selecting four sampling points to describe the upstream, mixing zone, and downstream water systems of the Euphrates River. The physicochemical properties of water at wastewater confluence sites indicated a hydrochemical uni-intrusion vortex behavior that was detected and confirmed by spatial variation of important indicators related to environmental applications, including (K, Na, Ca, Mg, HCO_3, SO_4, Cl, NO_3, PO_4, Temp., DO, BOD_5, NH_4, Turb., EC, pH, HT, and TDS). The distribution of dissolved oxygen (DO) in the Euphrates River was governed by a spatial enrichment gradient of 0.04 to 0.06 mg/L m. The distribution behavior of the DO plumes depends on the re-aeration process (K_2) at a rate ranging from 0.4 s^{-1} to 1.416 s^{-1} associated with the re-oxygenation process (K_1) ranging from 0.172 to 0.82 s^{-1}. Wastewater is considered to be a source of spot contamination with brackish water and emits chemical pollutants with a total dissolved discharge of 18,190 ton/y, which is the source of salinization in river water. The hydrochemical classification revealed the succession of different water facies developed by the intruding water of the Na-SO_4-chloride type in the freshening phases. According to the Canadian water quality index, water in the Euphrates River has been categorized as good water for aquatic life.

Keywords: Water quality; Re-aeration; Euphrates River; Pollution plume; Sewage

1. Introduction

River bodies are suffered from a potentially challenging situation due to the existence of a variety of variables that greatly intensify the case [1–3]. Water quality is directly related to water discharge, travelled distance, water depth, and dilution rates [4–7]. These ever-changing physical conditions in large rivers make it impossible to forecast hydrological processes [8,9]. Deep and persistent human activities in rivers had already contributed to system shifts and added new pollutants to the riparian environment [10,11]. Monitoring the impact of polluting water

* Corresponding authors.

Presented at the 8th International Conference on Sustainable Solid Waste Management (Thessaloniki 2021), 23-25 June 2021, virtual conference

flows is a critical step in evaluating the ecological degradation of rivers [4,12]. Furthermore, many researchers continue seeking to identify a reliable collection of flow metrics that accurately measure facets of the flow regime that must be maintained in order to preserve the stability and functionality of the river environment [13,14]. Among similar regional studies, Hikmat and Juwana [15] research deals with pollution loads from local sector sources in the Cisangkan River. Other studies concluded that municipal wastewater discharged into the Gumti River through sewage drains was responsible for higher trace elements values and demonstrated the influence of anthropogenic pollutants at a long distance in river water [15].

The Euphrates passes through three countries Turkey, Syria, and then Iraq. The basin of the river covers 440,000 km^2 of the three countries about 47% of this area is being grounded in Iraqi land. Several reports and studies were conducted for the study area, including previous geological reports for the Iraqi Geological Survey (GEOSURV) [16–18]. Hydrogeological studies; surface and groundwater resources [19–24]. Hydrochemical studies [25–28]. A statistical study was also carried out on the source and origin of the hydro-chemical components and the potential for pollution in the waters of the Euphrates River [29]. The mean daily discharge of the Euphrates River recorded in the Hit gauge station ranged between 550 and 7,460 m^3/s during the period (1958–1982). Also, 1,586 million tons of sediments were transported in the same period [25].

Iraq's surface and groundwater resources have suffered from critical contamination and erroneous management policies during the last 20 years. Water quality has become a crucial problem in the Euphrates River for several reasons. Return flows from agricultural drainage that causes salinity problems along the river course [11,12].

The goal of the current study is to determine the direct impact of municipal wastewater and sulfur springs on the freshwater body in the Euphrates River, Hit sector. It is also to calculate the amount of disposal load in the river water, estimate the degree of mixing and the coefficient of self-purification, and explore the behavior of the physicochemical components in the mixing plumes. Finally, assessing the water suitability for aquatic life.

1.1. Geological and hydrogeological study of the study area

The study area is located in the Hit City, Al-Anbar Governorate, Western Iraq. Some of the surface and groundwater from the valleys, streams, springs, agricultural, industrial, medical, municipal, and domestic waste flows directly into the Euphrates River. The primary uses of Euphrates water in the study area are for drinking and irrigation. Many human activities, such as cattle farms, crop-producing farms, and other agricultural lands, surround the riverside study area. During the field survey, three effective sites in the study area were identified (Fig. 1, Table 1).

1.1.1. Geological sitting

Tectonically, The Euphrates River, where it enters the Iraqi Territory from Syria, forms the contact between two tectonic zones, Al-Jazira and Western Desert zones. It passes through the Stable Shelf, then goes in its way, then enters the Mesopotamian Basin in Central and South Iraq. The river flows parallel to the only surface anticline (Anah Anticline) along the course of the river within the Iraqi Territory in W-E trend and continues until Haditha Town. There, it flows entirely within Al-Jazira Zone until west of Ramadi City (South of the study area). Thereafter,

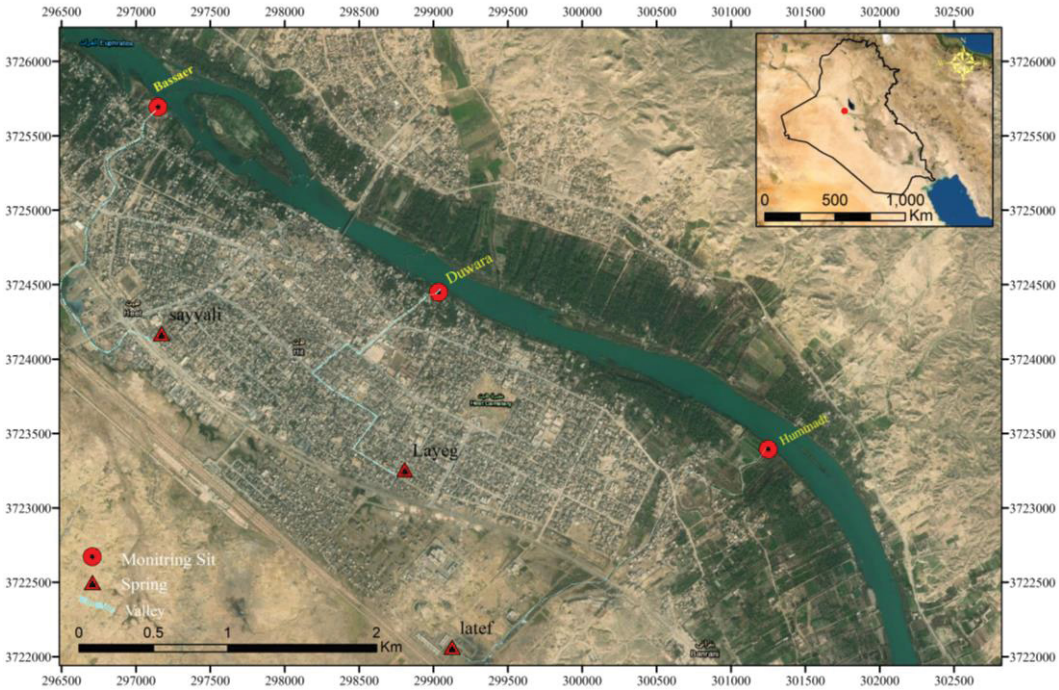

Fig. 1. Location map of the study area and monitoring sites.

Table 1
Coordinates the observation sites, river water levels

Station ID	Easting (m)	Northing (m)	Elevation (m)	Distance (m)	Hydraulic gradient	Remark
B	297143	3725691	56	0	(54.88–54.24)/ 4500 = 0.000142	Bassaer site
B1	297135	3725756				
B2	297229	3725670				
B3	297281	3725626				
D	299034	3724443	58	2,250		Duwara site
D1	298993	3724510				
D2	299060	3724488				
D3	299160	3724430				
H	301245	3723394	57	4,700		Hummadi site
H1	301195	3723454				
H2	301275	3723410				
H3	301330	3723360				

it flows in the Mesopotamian Zone and continues until it merges with the Tigris River. However, the Euphrates River within the Mesopotamian Zone flows almost parallel to the Abu-Jir Euphrates Fault Zone; between Al-Najaf and Al-Simawa Cities.

Geologically, geological layers play a significant role in determining the quality of Euphrates' water. The Euphrates River enters Iraq a few kilometers North of Huseiba Town in Al Qaim on the Iraq–Syria frontier. The river upper reaches in Iraq, cuts through carbonate bedrocks, having a very narrow strip of the flood plain. The lithology of the Euphrates River channel then changed to gypsum, limestone, green marl from North Hit to Ramadi [30,31]. In the Hit District, the river flows entirely within the rocks of the Fat'ha Formation (Middle Miocene). Between Hit Town and Al-Ramadi City, on the right side of the river, the rocks of the Nfayil Formation (Middle Miocene) are exposed. The formation consists of an alternation of green marl and limestone. In the middle and lower reaches the river meander over the Mesopotamian alluvial plain. The drainage basin here is underlined by the Injana Formation (Upper Miocene) which consists of marls and sandstone at south Ramadi [30]. At the lower reaches, the river flows over fluviatile recent sediments and the Dibdibba Formation (Miocene–Pliocene–Pleistocene) which is consists of clastic sediments. The exposed formations in the study area are shown in the geological map of Iraq (Fig. 3).

The lithostratigraphy in the study area can be described as follows: Euphrates Formation (Lower Miocene). It has widespread exposure extending towards the south and southwest within the Mesopotamian Plain until Falluja City. It mainly consists of limestone. This formation hosts the Euphrates River within the study area and adds calcium ions (Ca^{2+}) and carbonates ion (CO_3) due to dissolution processes. Fat'ha Formation (Middle Miocene) in the study area appears to be on the top of the stratigraphic succession forming Mesa and Cuesta landforms near the Hit area. The thickness of this formation is regionally variable from hundreds of meters to a few meters, but in the study area around Hit, it is less than (25 m), mainly consisting of gypsum and anhydrite interbedded with limestone, marl, and relatively fine-grained clastics. Important contemporaneous travertine and bitumen lenses, interbedded with basal green marls occur near Hit City. The travertine has large voids (occasionally containing sulfur crystals). The travertine beds interfingers with the surrounding evaporites of the Fat'ha Formation. The travertine cones may have formed in very shallow lagoons as a result of asphalt seepage and bacterial reduction of the basal gypsum beds of the formation producing fluids that deposited sinters [32,33]. Injana Formation (Upper Miocene) overlies Fat'ha Formation. It's exposed SE study area near Habbaniyah area around the Euphrates River. Quaternary deposits are comprised of Pleistocene and Holocene deposits. The Pleistocene deposit is heterogenous of fine pebbles consisting of quartz, chert, carbonate, and clay. Cement materials mainly are silica and secondary gypsum. Holocene deposit represents the valley fill sediments, residual soils, sabkha deposits, flood plains, and eolian deposits which formed the Euphrates flood plain near the Hit area.

The study and surrounding areas are characterized by gas hydration and associated features. Good examples are the gas and, oil and bitumen seepages in Hit, Hammadi, Abu-Jir, and Jabha areas. Numerous bitumen springs, sulfide spring waters, bitumen beds are located near the Hit area and. These features and deposits that occur along the N-S Abu-Jir Fault Zone are characterized by active asphalt seepages (Ain Jabha, Ain Abu-Jir, Ain Atalt, and Ain Hit "Sayali" Ain Ilateef) [32]. These phenomena are contribution of highly saline sulfurous water discharging from natural springs issued as a result of Abu-Jir deep-seated fault [16].

1.1.2. Hydrogeology of the study area

The course of the Euphrates in the Hit sector is subject to the effects of the dry desert climate, depending on the outputs of the hydrometeorological model [35]. The annual rates of rain, evaporation, and temperature ranged from (100 to 125) mm, (1,900 to 2,100) mm, (24 and 25) °C, respectively. This region is located within the Abu-Jir Fault Zone. It is an active subsurface fault during the late Mio-Pliocene Epoch (Late Neogene Period) extending

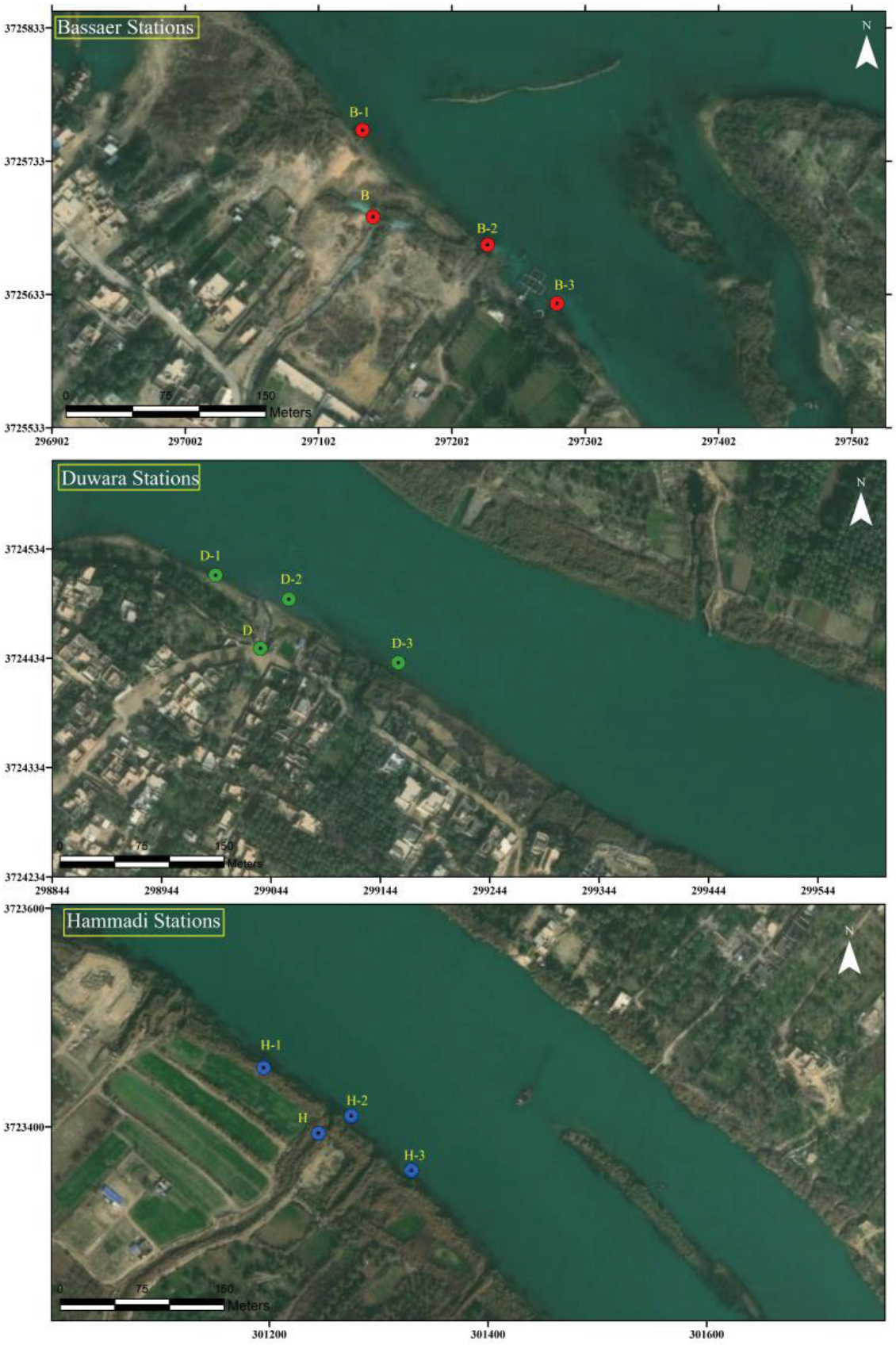

Fig. 2. Zoom in on study area location and monitoring sites (B, D, H).

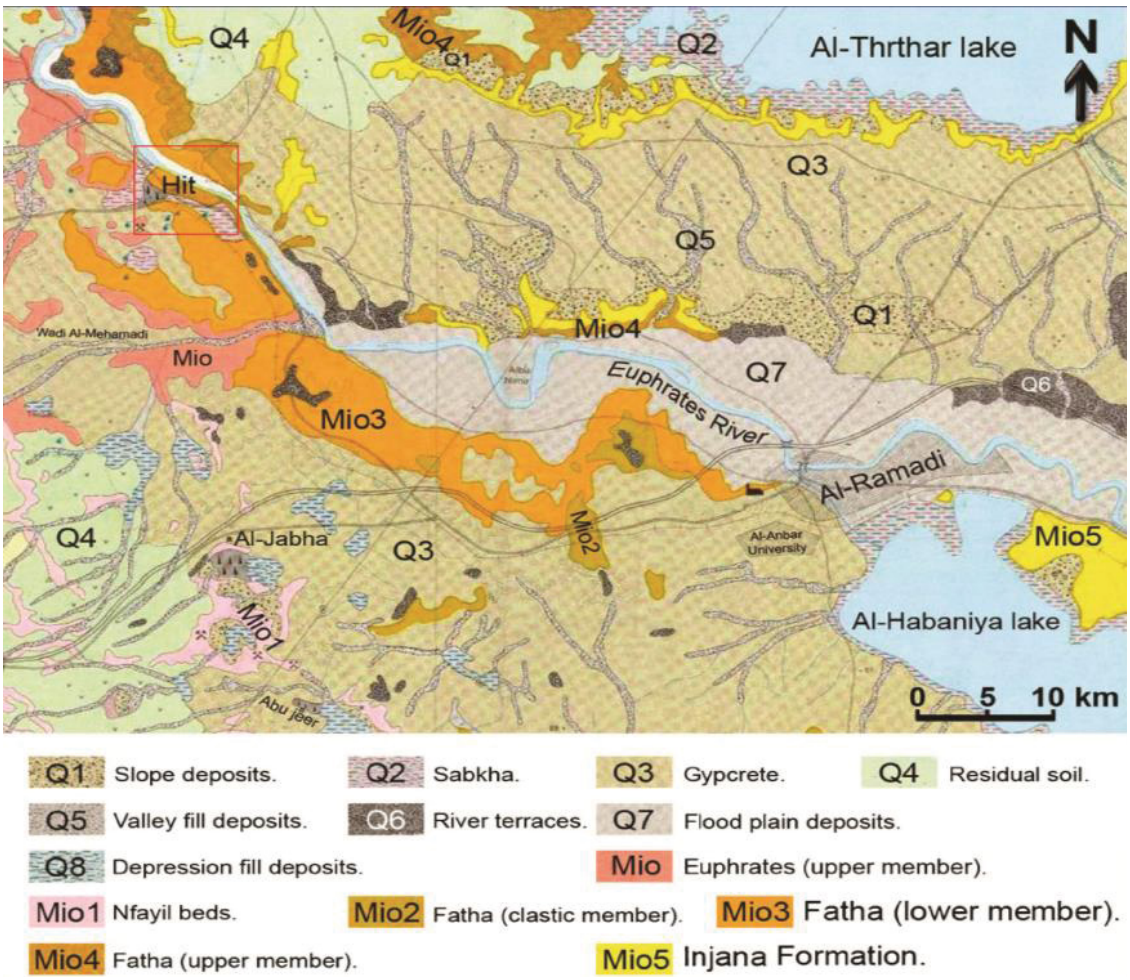

Fig. 3. Geological map of the study and surrounding area [34].

NW-SE. Limestone water-bearing with limited extensions of Fat'ha Formation was classified as perched aquifer of very low productivity, depending on their feeding from rainwater and on the deep source of spring water that flows on the rock surface [36]. The aquifer of the porous dolomitic limestone of the Euphrates Formation was classified as a semi-confined aquifer. The aquifer of the porous dolomitic limestone of the Euphrates Formation was classified as a semi-confined aquifer. The water-bearing layers of the quaternary sediments were characterized by bank storage conditions and play a regulatory role between the groundwater and the surface water of the Euphrates River. Salt chloride water flows from Sayala, Layeg, and Iltayif (locally names springs) at a level less than (70) m. a.sl. The water discharge of these springs was 35, 3, and 6 l/s, respectively [37]. Sayala spring water continuously flows in a stream toward the industrial district, then to Bassaer valley and mixes with municipal wastewater, and finally, flows into the Euphrates River at the site (B) as shown in Fig. 1. The water of the Layeg spring flows and mixes with the sewage in Hummadi valley to flow in the river at the site (H). As for the Iltayif spring water, it is mixed directly with municipal wastewater up to the final drainage site (D). The hydraulic gradient of the Euphrates River water level within the study area between Bassaer (B) and Hummadi (H) stations was 0.00014.

2. Methodology

The sampling process for Euphrates River water in the Hit sector was performed, taking into consideration the locations of municipal wastewater mixed with spring water flowing from different regions of the city (Fig. 1). The coordinates of the water samples points are precisely determined for sampling at each location using the GPS device (Table 1). These points are called Bassaer (B), Duwara (D), and Hammadi (H). The monitoring program was carried out with 9 labeled points (B1-B3, D1-D3, and H1-H3) (Table 1, Figs. 1 and 2). The polyethylene bottles were used to collect water samples (1.5 L).

Electrical conductivity (EC), total dissolved solids (TDS), the concentration of ion hydrogen (pH), temperature, and dissolved oxygen (DO) were measured immediately after sampling using a portable digital device. The major ions (HCO_3^-, CO_3^{-2}, SO_4^{-2}, Cl^-, NO_3^-, PO_4^{-3}, Ca^{+2}, Mg^{+2}, Na^+, K^+, NH_4^+, HT, and Turb.) have been analyzed using standard methods proposed by the American Public Health Association [38,39].

The analytical accuracy of all water samples (chemical composition) was determined using the formula charge balance method, expressed in Eq. (1). The accuracy of the water analysis looks to be within an acceptable value (5%).

$$U\left(\text{reaction error}\right)\% = \frac{\sum \text{Cations} - \sum \text{Anions}}{\sum \text{Cations} + \sum \text{Anions}} \times 100 \quad (1)$$

where (U) is the uncertainty.

Direct discharge (Q) is very important for predicting the transport of pollutants. Depending on the Brikowski procedure [40], Q was calculated from the velocity (V) and the cross-section of the stream according to Eq. (2).

$$Q\left(\frac{m^3}{\text{sec}}\right) = V\left(\frac{m}{\text{sec}}\right) \times A\left(m^2\right) \quad (2)$$

where the area of the cross-section is obtained by multiplying a width (m) by a depth (m).

The data obtained from the observations were used to identify the hydrochemical and environmental facts of the wastewater in the mixing zone of the Euphrates by monitoring a total of 342 different readings (Tables 2 and 3).

3. Results and discussion

3.1. Hydrochemical properties

The Euphrates River water in the study area was classified under a category of slight alkaline reaction with an average pH value of 7.2, fluctuating in a low significant level with an average of variability (Cv% = 3.8%) ranging between the values of (7.2 ± 0.28). According to the classification of water based on temperature [41], the river water characterized by being tepid water within a temperature ranging between 23°C and 25.5°C, fluctuated in a low significant level of 0.72°C, under a rate of variation of 2.95% among the monitoring points, influenced by Bassaer, Duwara, and Hummadi sewage temperature.

Table 2
Water velocity and discharge

Site	Station ID	Time (s)	Distance (m)	Velocity (m/s)	Depth (m)	Width (m)	Cross-section area (m^2)	Discharge (m^3/s)
Sewage	Bassaer	33	1	0.03	0.4	3	1.2	0.036
	Duwara	9	1	0.11	0.675	1.1	0.742	0.081
	Hummadi	40	1	0.025	0.65	1.5	0.975	0.024
Euphrates River	upstream B	11	2	0.18	1	10	10	1.8
	upstream D	10	4	0.4	1.5	5	7.5	3
	upstream H	10	3	0.3	2	12	9.6	19.2

Table 3
Physicochemical analyses of the Euphrates water and wastewater at B-H3

Station ID	B	B1	B2	B3	D	D1	D2	D3	H	H1	H2	H3
Parameters												
pH	6.0	7.4	6.6	7.4	5.5	7.3	6.8	7.2	7.2	7.4	7.3	7.2
Temp. (°C)	25.0	24.0	24.5	24.0	26.0	25.0	25.5	25.0	25.0	23.0	24.0	25.0
Turb. (mg/L)	17.0	3.6	4.1	2.6	33.0	9.2	11.0	7.1	11.0	7.3	10.0	6.4
HT (mg/L)	1,565	278	280	280	1,329	248	349	371	2,257	291	297	294
BOD (mg/L)	7.0	3.4	3.5	2.5	5.2	1.6	4.0	2.0	2.6	0.2	1.4	1.5
DO (mg/L)	1.1	7.0	6.1	8.0	1.3	8.6	3.8	6.0	8.1	9.4	7.6	7.7
K (mg/L)	64.0	3.0	4.9	3.1	41.0	3.2	6.7	6.0	77.0	3.1	3.0	1.4
Na (mg/L)	911	44	61	44	688	47	85	81	1,213	43	47	85
Mg (mg/L)	157	27	28	27	128	26	31	30	180	28	30	28
Ca (mg/L)	368	66	68	67	322	70	88	86	607	71	73	72
Cl (mg/L)	1,940	113	134	116	1,314	102	177	151	2,811	76	81	78
SO_4 (mg/L)	688	165	186	168	561	177	234	229	798	166	172	170
HCO_3 (mg/L)	315	118	126	120	214	137	154	151	277	122	133	126
NH_4 (mg/L)	0.21	0	0.05	0.11	0.00	0.00	0.00	0.00	0.19	0.09	0.09	0.00
PO_4 (mg/L)	0.05	0.00	0.05	0.00	0.05	0.00	0.05	0.00	0.0	0.00	0.05	0.00
NO_3 (mg/L)	17.0	5.0	8.0	7.0	33.0	13.0	16.0	11.0	36.0	8.0	11.0	6.0
TDS (mg/L)	4,517	508	545	536	3,254	563	776	734	6,011	509	539	521
EC (μS/cm)	6,400	630	735	620	4,180	911	1,000	681	9,810	670	698	653

Depending on the concentration of TDS and according to the salinity classification [42], the river water is classified as freshwater, where TDS values ranged between 508 and 776 mg/L, with a fluctuation value of 94.84 mg/L at a variability rate of 16.31%. This variation reflects the effect of mixed municipal and springs water discharge, which is classified as brackish water (TDS; from 3,451 to 6,011 mg/L).

The waters of the Euphrates are not suitable for industrial purposes, as the values of total hardness ranged from 278 to 371 mg/L. It is very hard water, according to the hardness classification [43]. More specifically, its values ranged from 278 to 280 mg/L, from 248 to 371 mg/L, and from 291 to 298 mg/L nearby the sewage disposal sites of Bassaer, Duwara, and Hummadi, respectively.

The concentration values of DO, biochemical oxygen demand (BOD_5), and NO_3 of the Euphrates water revealed no serious contamination status, with rates of their concentrations reaching 7.1, 2.2, and 9.4 mg/L, respectively. The serious pollution status was only observed near the Bassaer and Duwara sewage disposal sites. It is caused by the presence of biodegradable substances in wastewater, as it was characterized by a low concentration of DO (<6 mg/L) accompanied by a relatively high concentration of BOD_5 (>3 mg/L) and NO_3 (>10 mg/L). In addition to the wastewater intrusion zone at the Hummadi site concerning nitrate concentration (NO_3, >10 mg/L).

Cations and anions concentration of the river water within the Hit sector fluctuated at values ranging from 1.38 to 15.65 mg/L and from 12.39 to 32.85 mg/L, respectively. Whereas, the values of variance rates ranged from 5.5% to 34.5% and from 9.4% to 28.76%, respectively. The variation in the concentration of ions is attributed to the mechanism of mixing-dilution related to the dissolved disposals from wastewater and the behavior of recovering the concentration of its components due to the higher discharge of the river compared to the effluent flows at the three sites.

The phenomenon of fluctuation in the quality of the Euphrates River within the study area can be summarized by revealing the values of the physical and chemical variables as measured in nine observation points (Figs. 5 and 6).

As it showed clear fluctuations, ranging between the values of (M+SD) and (M-SD) for each variable (Table 3) and high peaks associated with the wastewater disposal sites in Bassaer, Duwara, and Hammadi, expressing the response of the river's water quality to the effects of wastewater components, especially in Duwara sewage disposal site.

The indicators also showed a decrease in their values in the sectors between sewage disposal sites to reach their background values due to the process of dilution and mixing and the river's ability to recover the concentration of its components due to diffusion and dispersal processes.

3.2. Statistical characterization of the pollution plumes at the sewerage confluence zone

A practical field monitoring program was implemented to obtain water quality data within the mixture of municipal wastewater and the Euphrates water, including the sewage disposal of Bassaer, Duwara, and Hummadi sites. The monitoring sites were selected based on the solutes flux as a point source pollution due to its addition of important chemical components concentration to the Euphrates River. Comparisons were made among the pollution indicators according to the Spearman correlation coefficient (Table 4), and the statistical results showed the following facts:

- The presence of a highly correlated direct relationship between the concentrations of the physicochemical variables as indicators of pollution, including (TDS, K, Na, Ca, Mg, Cl, SO_4, HCO_3, NO_3, and Temp.), confirming the phenomenon of simple linear mixing, based on mono-distribution interference within the water body.
- The presence of direct relation with low correlation between both concentration of ammonium (NH_4) and phosphate (PO_4), and the rest of the variables, mainly confirmed their source to wastewater affected by dilution process.

Table 4
Statistical comparison of pollution indicators (Spearman correlation coefficient)

Indicator	TDS	K	Na	Mg	Ca	Cl	SO_4	HCO_3	NO_3	NH_4	Temp.	pH	PO_4	DO
TDS	1.0													
K	0.88	1.0												
Na	0.92	0.78	1.0											
Mg	0.77	0.43	0.79	1.0										
Ca	0.71	0.49	0.75	0.87	1.0									
Cl	0.87	0.70	0.83	0.71	0.49	1.0								
SO_4	0.98	0.82	0.94	0.82	0.74	0.87	1.0							
HCO_3	0.95	0.82	0.88	0.83	0.83	0.76	0.96	1.0						
NO_3	0.94	0.86	0.81	0.76	0.74	0.73	0.91	0.93	1.0					
NH_4	0.18	0.07	0.37	0.41	0.35	0.28	0.24	0.24	0.1	1.0				
Temp.	0.75	0.68	0.67	0.52	0.50	0.64	0.77	0.77	0.68	0.007	1.0			
pH	–0.7	–0.5	–0.7	–0.6	–0.5	–0.7	–0.8	–0.7	–0.6	–0.07	–0.70	1.0		
PO_4	0.65	0.54	0.54	0.63	0.47	0.66	0.65	0.70	0.66	0.26	0.74	–0.3	1.0	
DO	–0.5	–0.2	–0.5	–0.4	–0.2	–0.3	–0.5	–0.47	–0.3	–0.07	–0.48	0.78	–0.35	1.0

- There is an inverse correlation relationship between both pH and DO values and the concentrations of other indicators, as it revealed the active effect of municipal wastewater mixed with spring water, which was characterized by high concentrations and decrease in DO concentration with pH values related to the degree of solubility.

3.3. Hydrochemical classification of the Euphrates water and the sewage water

A statistical distribution chart [44] was applied for characterizing the quality of river water and wastewater using the data of the main hydrochemical ions analyzes (Fig. 4). The river water at all monitoring points before and after the sewage disposal site in Bassaer (B1, B3), Duwara (D1, D3), and Hummadi (H1, H3), was classified as a sulfate group, at the category of calcium–sulfate Family represented by (Na-Ca; Cl-HCO_3-sulfate) water type. The water of the mixture plume with the river water at the sewage disposal site in Bassaer (B2) and Hummadi (H2) was classified as a water type of (Na-Ca; HCO_3-Cl-sulfate), While the sewage water at the confluence site of Duwara (D2) has a water type of (Ca-Na; HCO_3-Cl-sulfate). Those water types reveal the behavior of moderate hydrodynamic activity affected by the intrusion of a mixture of municipal wastewater and effluent spring water. The sewage water was characterized by Na-SO_4-chloride type in the three sites. The hydrochemical facies (Fig. 4) illustrated the succession of different water facies developed between intrusion (Na-SO_4-chloride type) and freshening phases, followed by the evolution of Na-Ca; HCO_3-Cl-sulfate and Ca-Na; HCO_3-Cl-sulfate, to be mixture water by a slight intrusion.

3.4. Pollutant load and mixing mechanism at the sewage disposal sites

The water of the Euphrates is exposed to the hazards of chemical pollution resulting from mixed flows of municipal wastewater and salty springs. The degree of river degradation was calculated by the daily discharge of pollutants into the Euphrates, using the flux-based algorithm according to the measures of instant discharge and concentration [45,46].

The discharge of the daily pollutant load added to the river at Bassaer, Duwara, and Hummadi disposal sites reached 13.922 ton/d with a total annual load of 5,128 ton/y, 23.33 ton/d with a total annual load of 8,515 ton/y, and 12.46 ton/d with a total annual load of 4,548 ton/y, respectively (Table 5). The percentage of anions and cations that added to the river from the disposal sites are ranged between 66.5% and 33.5%, respectively.

The rate of mixing ions between the Euphrates water and the sewage in the disposal sites was calculated using the chloride ion concentration [47] as shown in Eq. (3).

$$R\% = \left\{ \frac{\left[Cl_{\text{mixing plume}} \right] - \left[Cl_{\text{upstream}} \right]}{\left[Cl_{\text{wasewater}} \right] - \left[Cl_{\text{mixing plume}} \right]} \right\} \times 10 \quad (3)$$

where $Cl_{\text{mixing plume}}$: represent the chloride concentration of the plume mixed water, Cl_{upstream}: represents the chloride concentration of the Euphrates water before mixing, and $Cl_{\text{wastewater}}$: represents the concentration of the chloride in wastewater.

The chloride concentration is used because it is the least affected by the chemical reactions in the aquatic environment [48] The mixing rate (R%) at the disposal site of Bassaer, Duwara, and Hummadi reached 1.2%, 6.6%, and

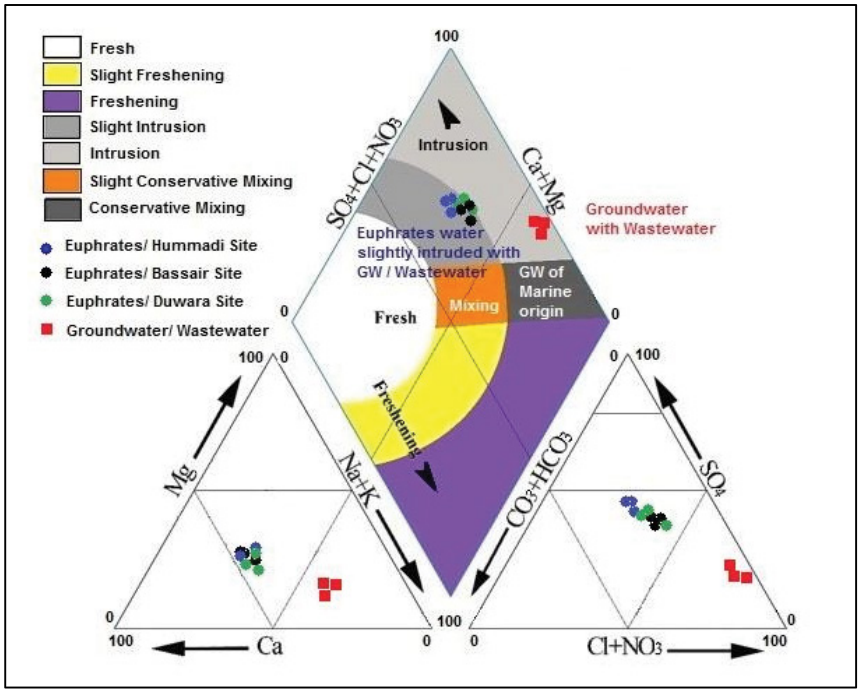

Fig. 4. Classification of the Euphrates water and wastewater quality on the adopted Piper chart.

Table 5
Daily and annual disposed loads to the Euphrates River

Variables	Bassaer site		Duwara site		Hummadi site	
	Load (ton/d)	Contaminants load (%)	Load (ton/d)	Contaminants load (%)	Load (ton/d)	Contaminants load (%)
K	0.199	1.429	0.289	1.238	0.160	1.284
Na	2.833	20.349	4.815	20.635	2.515	20.185
Mg	0.488	3.505	0.896	3.84	0.373	2.994
Ca	1.144	8.217	2.253	9.655	1.258	10.097
Cl	6.033	43.334	9.195	39.405	5.827	46.768
SO_4	2.139	15.364	3.926	16.825	1.654	13.275
HCO_3	0.979	7.032	1.498	6.419	0.574	4.607
NO_3	0.053	0.38	0.231	0.990	0.075	0.601
PO_4	0.0002	0.0014	0.0004	0.0017	0	0
NH_4	0.0007	0.005	0	0	0.0004	0.003
TSS	0.053	0.380	0.231	0.990	0.023	0.184
Daily total load (ton/d)	13.922		23.33		12.46	
Annual load (ton/y)	5128		8515		4548	

0.2%, respectively. This means that 98.8%, 93.4%, and 99.8% of the ion's concentration are derived from the sewage, emphasizing the danger of the mixed water to the aquatic environment and health, classifying it as pollution source.

3.5. Spatial distribution of the physicochemical variables

Water pH values are affected by the types of dissolved substances depending on the oxidation and reduction reactions [49], including reactions influenced by the concentration of dissolved oxygen associated with the degree of aeration and/or reactions associated with photosynthesis and respiration [50,51].

Fig. 5 shows a pH distribution map for the Euphrates water where its pH value ranged between 7.2 and 7.4 within the Hit sector. The river water in the mixing zone of Bassaer and Duwara disposal sewage sites was classified as being slight-acid water with a pH rate of 6.6 and 6.8, respectively, affected by the acidity of the sewage intrusion at a pH value equal to 6 and 5.5, respectively.

Then the river water recovered the value of pH, as it was detected at the site located upstream of the river. The mixing process (dispersion mechanism) occurred with a spatial pH gradient value ranging between 0.02 and 0.08 (pH-meters). This phenomenon was not recorded at the Hummadi site due to the mixing of sewage water with Iltayif spring water, which is classified as slight alkaline water (with a pH value of 7.2).

Fig. 6 shows the phenomenon of temperature distribution in the Euphrates water. It ranged between 23.5°C and 24.5°C. A plume of slight thermal pollution was observed at the sewage disposal sites (water temperature; 24.8°C–25.5°C), due to the sewage intrusion at a temperature of 25°C–26°C. The effective distance of the heat flux ranged between 75 to 200 m, which was controlled by a thermal gradient ranging from 0.004 to 0.012°C/m.

The distribution map of the total suspended solids (TSS) in the Euphrates water (Fig. 7) revealed an increase in their concentrations near the bank, which ranged between 5 to 6 mg/L, due to the effect of the waves and their leaching process on the bank sediment.

Also, a significant increase was recorded near the wastewater disposal sites, whose value ranged between 10 and 30 mg/L. The Euphrates water is affected by the turbidity of the wastewater (11–33 mg/L). Low concentration was recorded at values less than 10 mg/L offshore. Results of comparing the concentration of TSS with water quality standards indicated unacceptable limits to aquatic life in sewage discharge sites and are useless to municipal supplies before treatment.

The TDS distribution map (Fig. 8) showed a clear differentiation between sewage and river water. The value of the TDS concentration was between 3,254 and 6,011 mg/L in wastewater and <600 mg/L in river water.

It also detected high concentrations of TDS near the riverbank of shallow depth affected by the waves and their chelation to the deposits of the bank in addition to the disposals of the wastewater. The process of dispersion between the pollution sources and the end of pollution plumes caused by the velocity of the river takes place under the influence of the dilution coefficient (dc/dx) of 22–39 mg/L m.

3.6. Spatial analyses of the environmental indicators (behavior and characterization)

Physicochemical variables such as DO, BOD_5, and NO_3 were used to identify the hydrochemical behavior of the Euphrates River in the Hit sector, taking into account the effect of sewage water at its disposal sites. The results of the spatial distribution maps of these variables were adopted as indicators in explaining the phenomena related to the dilution process and determining the pollution plumes and their dispersion extent. The re-aeration coefficient K_2 (time^{-1}) which is an important environmental parameter for determining the rate of self-purification was calculated, using Eq. (4) [52,53].

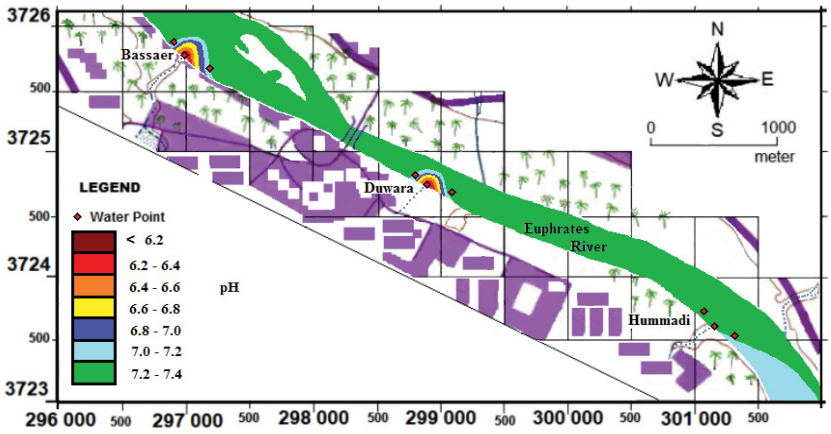

Fig. 5. pH distribution map within the Euphrates water.

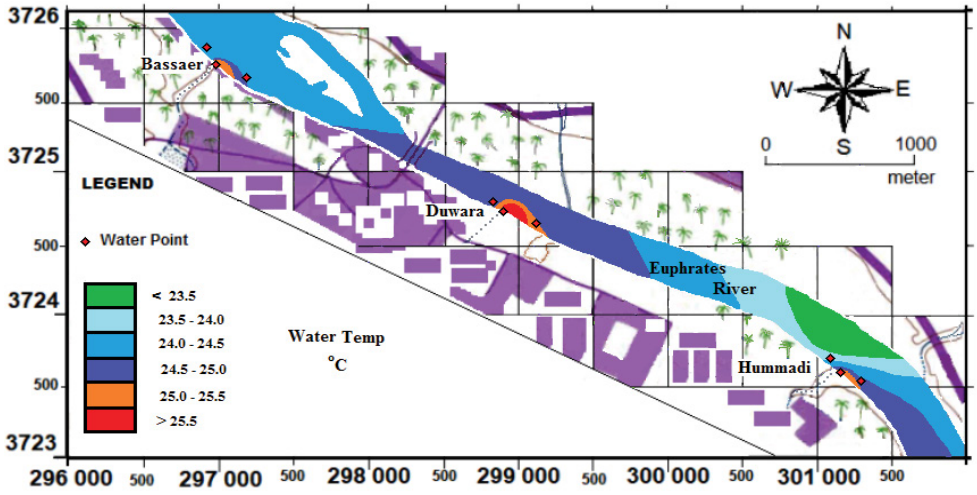

Fig. 6. Temperature distribution map within the Euphrates water.

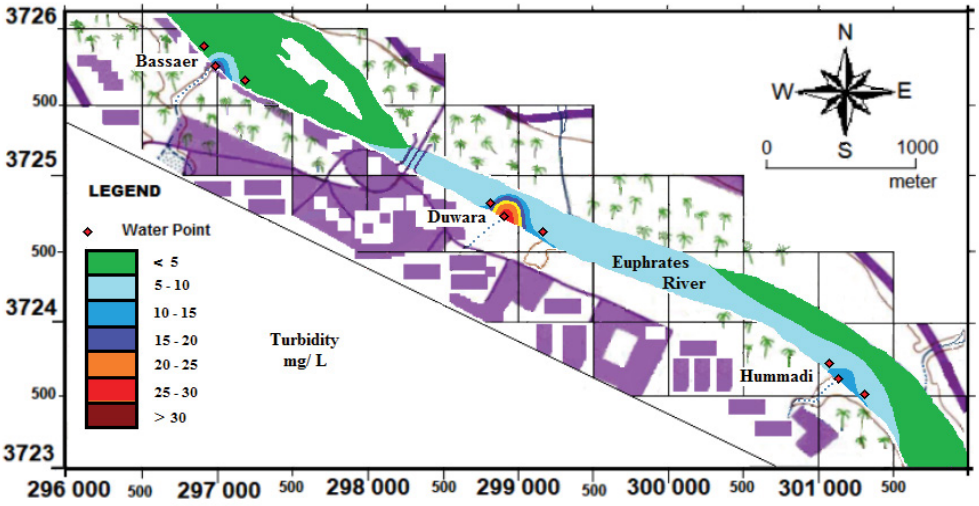

Fig. 7. TSS distribution map within the Euphrates water.

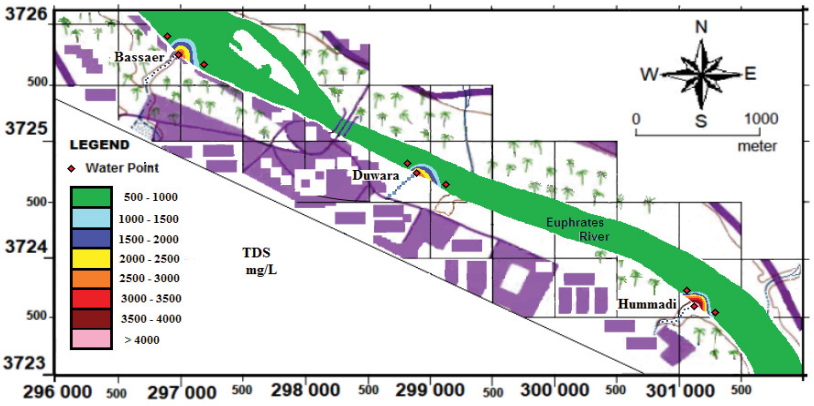

Fig. 8. TDS distribution map within the Euphrates water.

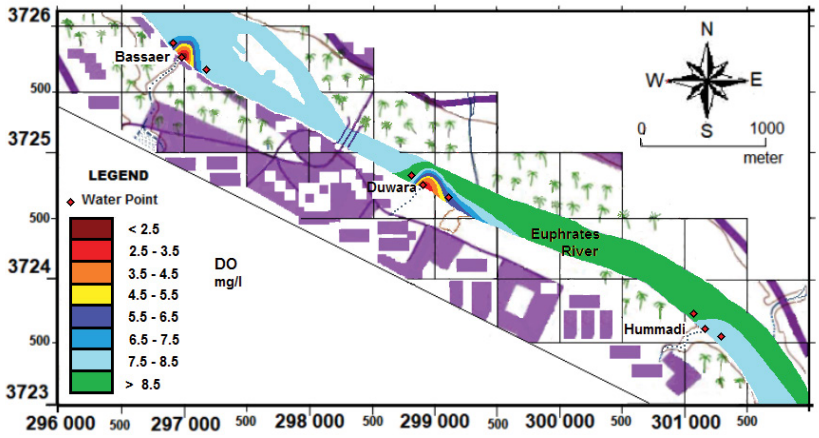

Fig. 9. DO distribution map within the Euphrates water.

$$K_2 = \left[\frac{\left\{ 0.065\left(\text{wind velocity}\right)^2 + 3.86\left[\frac{\text{water velocity}}{\text{water depth}} \right]^{0.5} \right\}}{\text{Water depth}} \right] \quad (4)$$

where K_2 = [0.0659 (wind velocity)^2 + 3.86{(water velocity)/(water depth)}$^{0.5}$]/water depth. Wind velocity ranged from 0.8 to 1.2 m/s. Water velocity ranged from 0.18 to 0.4 m/s. Water depth ranged from 1.5 to 2 m.

The concentration of DO in the Euphrates water within the Hit sector was greater than 6.5 mg/L (Fig. 9). Two plumes of DO deficiency (<6.5 mg/L) were detected at the confluence sites of the Bassaer and Duwara with the Euphrates River, caused by sewage intrusions (DO concentration <2 mg/L). The dissolved oxygen concentration increased by a spatial enrichment gradient of 0.04–0.06 mg/L m in the last part of the plumes with a re-aeration rate (K_2) of 0.4–1.416 s^{-1}, up to a recovery concentration of 7 mg/L as observed in river water before mixing. The re-aeration process is proportional to the difference between the saturation concentration DO_{sat} and the observed DO concentration due to external inputs of oxygen from the atmosphere.

The majority of river water was characterized by a low concentration of BOD_5 (<2.5 mg/L), except near the sewage-disposal sites (Fig. 10), which revealed an opposite distribution phenomenon of the DO concentration. The BOD_5 concentration decreased from 7 mg/L in the sewage to a recovery concentration of 2.5 mg/L with a spatial dilution gradient of 0.04 mg/L m, due to the re-aeration process followed by the mixing/dilution mechanism with the flux direction.

Comparing the BOD_5 values with the water quality standard (2.5 mg/L), the mixture water of the plume is somewhat bad for aquatic life and is not recommended for drinking.

The Euphrates water is dominantly characterized by a concentration of NO_3 less than the permissible drinking limit (10 mg/L). Pollution plumes of nitrate were detected near the Bassaer, Duwara, and Hummadi sewage-disposal sites with a distance less than 41, 80, and 100 m, respectively from the source of pollution.

The nitrate concentration of the pollution plumes ranged from 10 to 17 mg/L, from 13 to 33 mg/L, and from 12 to 36 mg/L (Fig. 11), originating from the anthropogenic domestic and natural springs additions of nitrate. The high concentration is due to the bacterial nitrification process in the presence of organic matter in sewage water [49,54]. On the other hand, the concentration of phosphate was not recorded above the limits of the laboratory analysis except

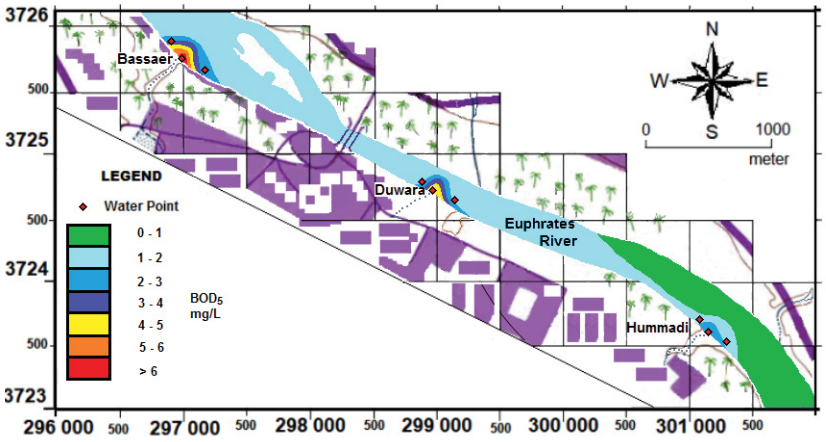

Fig. 10. BOD_5 distribution map within the Euphrates water.

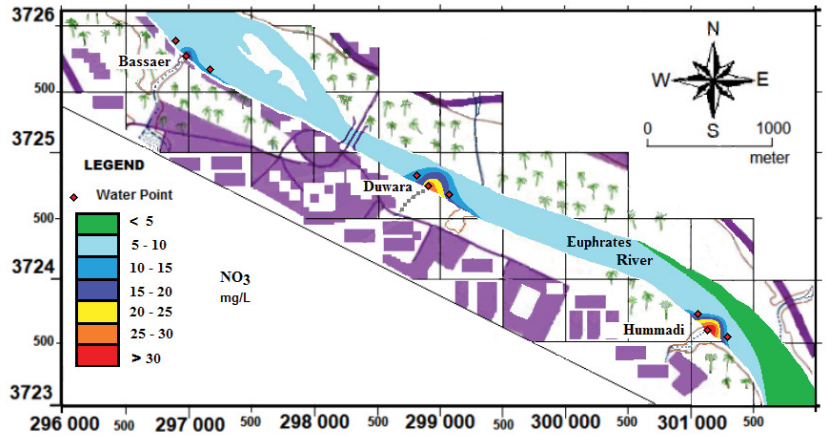

Fig. 11. Nitrate distribution map within the Euphrates water.

for its concentration in the wastewater of 0.05 mg/L, which is less than the permissible limit (0.1 mg/L).

3.7. Self-purification factor

The concentration dispersion model (BOD_5, DO) with the direction of river flow [55] after pollutant discharge at sewage disposal has been described in Eqs. (5)–(8).

$$D_t = C_s - C \tag{5}$$

where D_t is dissolved oxygen deficiency, C_s is saturated DO concentration (mg/L), C is observed DO concentration at the downstream, extracted from the DO plume (Fig. 9).

$$\frac{\delta D_t}{\delta t} = k_1 b_t - k_2 D_t \tag{6}$$

where b_t is concentration of BOD_5 for the mix at the discharge point extracted from the BOD_5 distribution plume (Fig. 10), k_1 is the de-oxygenation factor (s^{-1}). δ_t – time (s) = distance of mixing(m)/water velocity (m/s).

$$k_1 = \frac{\left[\left(\frac{\delta D_t}{\delta t}\right) + k_2\right]}{b_t} \tag{7}$$

After integration Eq. (6) gives (f) = self-purification factor, which is marked by Eq. (8) [56–58].

$$f = \frac{k_2}{k_1} \tag{8}$$

Using Eqs. (1)–(3) and the data extracted from DO and BOD_5 distribution maps; the self-purification factor values within the pollution plumes at the Bassaer, Duwara, and Hummadi sewage-disposal sites reached 2.99, 1.72, and 2.32, respectively. These results indicated that the role of the re-aeration process (depends on water temperature, river speed, and depth) is higher than the re-oxygenation process (depends on the pollutant properties and the organic materials) by 299%, 172%, and 232%, respectively.

3.8. Application of the water quality index and health of ecosystems (aquatic environment)

Canadian Water Quality Index (CCME WQI) of a nine-point scale was used to summarize results from different 16 physicochemical measurements. The used parameters are pH, TDS, HT, K, Na, Mg, Ca, Cl, SO_4, HCO_3, DO, BOD_5, NO_3, Turb., NH_4, and PO_4 (Table 6). This index reduces huge amounts of data to a single, number thus ranking water into

Table 6
Data used in water quality index calculation for aquatic life

Station ID	pH	TDS (mg/L)	HT (mg/L)	DO (mg/L)	BOD_5 (mg/L)	NO_3 (mg/L)	Turb. (mg/L)	NH_4 (mg/L)	PO_4 (mg/L)	K (mg/L)	Na (mg/L)	Mg (mg/L)	Ca (mg/L)	Cl (mg/L)	SO_4 (mg/L)	HCO_3 (mg/L)
B3	7.4	536	280	8	2.5	7	2.6	0.11	0	3.1	44	27	67	116	168	120
B2	6.6	545	280	6.1	3.4	8	4.1	0.05	0.05	4.9	61	28	68	134	186	126
B1	7.4	508	278	7	3.5	5	3.6	0	0	3	44	27	66	113	165	118
D3	7.2	734	371	6	2	11	7.1	0	0	6	81	30	86	151	229	151
D2	6.8	776	349	3.8	4	16	11	0	0.05	6.7	85	31	88	177	234	154
D1	7.3	563	248	8.6	1.6	13	9.2	0	0	3.2	47	26	70	102	177	137
H3	7.2	521	294	7.7	1.5	6	6.4	0	0.05	3	46	28	72	78	170	126
H2	7.3	539	297	7.6	1.4	11	10	0.09	0	3.1	47	30	73	81	172	133
H1	7.4	509	291	9.4	0.2	8	7.3	0.09	0	3	43	28	71	76	166	122
Objectives	6.5–9	1,000	500	5	3	10	30	0.2	0.1	–	200	30	75	250	500	200

one of five categories, these are poor water (0–44), marginal (45–59), fair (60–79), good (80–94), and excellent quality of the sampled water (95–100) [22,59].

The values of the various scopes (F_1), frequencies (F_2), and amplitudes (F_3), with their respective water quality index in all nine river stations are listed:

- F_1 = (Number of failed variables/Total number of variables) × 100, =(5/16) × 100 = 31.25;
- F_2 = (Number of failed tests/Total number of variables) × 100, =(11/144) × 100 = 7.64;
- Σ_1^n excursion$_i$ = (Failed test value$_i$/Objective$_j$) – 1 = 2.396;
- nse = (Σ_1^n excursion$_i$)/Number of tests;
- nse = (2.396)/144 = 0.017;
- F_3 = nse/{0.01 nse + 0.01} = [0.017/{0.01 (0.017) + 0.01}] = 1.672;
- CCME WQI = 100 – [$\sqrt{\{(F_1)^2 + (F_2)^2 + (F_3)^2\}/1.732}$] = 100 – [$\sqrt{\{(31.25)^2 + (7.64)^2 + (1.672)^2\}/1.732}$] =81.4 (Good category).

Accordingly, the water quality of the Euphrates River is rated as good water for aquatic life (healthy ecosystem).

4. Conclusion

The study dealt with the extent of the confluence of two types of water with an active hydrodynamic behavior during the monitoring period. The water miscibility process calculated from the concentration of chloride in the deterioration zone of the pollution plume showed that 93.4%–98.8% of the chloride is due to its concentration in wastewater and 1.2%–6.6% due to its concentration in the Euphrates River. The dissolved load of the sewage was dispersed within the deterioration zone between the source of pollution and the recovery zone, in a mixing rate of water <2.7% from the sewage, and >97.3% originating from the Euphrates. The discharge load values of sewage pollutants ranged from 12.46 to 23.33 ton/d, with a total annual rate ranging from 4,548 to 8,515 ton/y, which represents the source of salinization in the river water. The scope of the pollution plumes has been spatially determined by employing the concentration of enrichment or dilution in the concentration of the indicators within the mixing zone. The effective axis of the pollution plume of Bassaer, Duwara, and Hummadi sites ranged from 40 to 50 m, 50–80 m, and from 200 to 250 m, respectively. The transport rate of the dissolved components, represented by the chemical gradient (dc/dx) of the TDS concentration, ranged between 22 and 39 mg/L m, along with the direction of the river flow.

Maps of pollution indicators and concentration of ions revealed the occurrence of a chemical mixing process with a uni-intrusion vortex of high concentration in the river freshwater, causing homogenous changes in distribution. The variation in the concentration of ions is caused by the mechanism of dilution and the mixing related to the sewage disposals in addition to the behavior of the concentration recovery balance, due to the higher discharge of the river compared to the low flow of wastewater. A significant increase in TDS and TSS concentration was detected near the riverbank of shallow depth affected by the river waves and weathering process in addition to the disposals of the wastewater. The application of the hydrochemical classification indicated the succession of different water facies developed by intruded water of Na-SO_4-chloride type in freshening phases, followed by the evolution of Na-Ca;

HCO_3-Cl-sulfate and Ca-Na; HCO_3-Cl-sulfate, to be mixed water by a slight intrusion. Those water types reveal the behavior of moderate hydrodynamic activity affected by a mixture of domestic wastewater and springs water. Since the sewage mixes with the river, the water of the pollution plume cannot be used for irrigation and drinking purposes.

Acknowledgments

The authors want to express their heartfelt appreciation for Prof. Bayan Muhie Hussien's substantial contribution to this study. Prof. Hussien passed away during the final stages of this project (may his soul rest in peace).

References

[1] Z. Wu, D. Zhao, J.P.M. Syvitski, Y. Saito, J. Zhou, M. Wang, Anthropogenic impacts on the decreasing sediment loads of nine major rivers in China, 1954–2015, Sci. Total Environ., 739 (2020) 139653, doi: 10.1016/j.scitotenv.2020.139653.
[2] M.A. Rabeea, A.S. Al-Rawi, O.J. Mohammad, B.M. Hussien, The residual effect of fish farms on the water quality of the Euphrates River, Iraq, Egypt. J. Aquat. Biol. Fish., 24 (2020) 549–561.
[3] M.A. Rabeea, A.J.R. Al-Heety, M.I. Mohammed, A.M. Fayydh, M. Elhag, Impact of Hijlan Creek springs on water quality of the Euphrates River and the hydrochemical characterization of the contamination plumes, Environ. Earth Sci., 80 (2021) 481, doi: 10.21203/rs.3.rs-338406/v1.
[4] S.M. Yarnell, E.D. Stein, J. Angus Webb, T. Grantham, R.A. Lusardi, J. Zimmerman, R.A. Peek, B.A. Lane, J. Howard, S. Sandoval-Solis, A functional flows approach to selecting ecologically relevant flow metrics for environmental flow applications, River Res. Appl., 36 (2020) 318–324.
[5] M. Mokarram, A. Saber, V. Sheykhi, Effects of heavy metal contamination on river water quality due to release of industrial effluents, J. Cleaner Prod., 277 (2020) 123380, doi: 10.1016/j.jclepro.2020.123380.
[6] T.A. Wallace, S. Gehrig, T.M. Doody, A standardised approach to calculating floodplain tree condition to support environmental watering decisions, Wetlands Ecol. Manage., 28 (2020) 315–340.
[7] B.M. Hussien, M.A. Rabeea, M.M. Farhan, Characterization and behavior of hydrogen sulfide plumes released from active sulfide-tar springs, Hit-Iraq, Atmos. Pollut. Res., 11 (2020) 894–902.
[8] J. Rodríguez-Estival, M.E. Ortiz-Santaliestra, R. Mateo, Assessment of ecotoxicological risks to river otters from ingestion of invasive red swamp crayfish in metal contaminated areas: use of feces to estimate dietary exposure, Environ. Res., 181 (2020) 108907, doi: 10.1016/j.envres.2019.108907.
[9] M.C. Thoms, T. Rose, F.J. Dyer, Riverine landscapes, water resource development and management: a view from downunder, River Res. Appl., 36 (2020) 505–511.
[10] X. Sun, D. Fan, M. Liu, H. Liao, Y. Tian, Persistent impact of human activities on trace metals in the Yangtze River Estuary and the East China Sea: evidence from sedimentary records of the last 60 years, Sci. Total Environ., 654 (2019) 878–889.
[11] H.N. Mukhlif, M.A. Rabeea, B.M. Hussien, Characterization of the groundwater within regional aquifers and suitability assessment for various uses and purposes-Western Iraq, Baghdad Sci. J., 18 (2021) 670–686.
[12] B.M. Hussien, M.A. Rabeea, H.N. Mukhlif, Estimation of corrosion and encrustation from groundwater chemistry of the aquifers: a case study of Al Hammad zone, Environ. Nanotechnol. Monit. Manage., 14 (2020) 100334, doi: 10.1016/j.enmm.2020.100334.
[13] C. Zhang, D. Tian, X.H. Yi, T. Zhang, J. Ruan, R. Wu, C. Chen, M. Huang, G.G. Ying, Occurrence, distribution and seasonal variation of five neonicotinoid insecticides in surface water and sediment of the Pearl Rivers, South China, Chemosphere, 217 (2019) 437–446.
[14] W. Wang, W. Li, Y. Yan, B. Liu, T. Wang, S. Mao, L. Song, H. Dou, W. Ao, C. Zou, Organic matter pollution during the Spring Thaw in Hulun Lake Basin: contribution of multiform human activities, Bull. Environ. Contam. Toxicol., 105 (2020) 307–316.
[15] R.R. Hikmat, I. Juwana, Pollution load of Cisangkan River: the domestic sector, IOP Conf. Ser.: Earth Environ. Sci., 277 (2019) 012029, doi: 10.1088/1755-1315/277/1/012029.
[16] M. Abbas, H. Al-Khatib, Complex Geophysical Interpretation of Hit Abu-Jir Shithatha Area, GEOSURV Lib., Report, 1982.
[17] V. Sissakian, S. Salih, The Geology of Ramadi Area. Map NA389 (GM18) Scale 1: 25000, GEOSURV, Unpublished Internal Report, 1994 (in Arabic).
[18] S.F. Fouad, Contribution to the structure of Abu-Jir Fault Zone, west Iraq, Iraqi Geol. J., 32 (2004) 63–73.
[19] S.M. Awadh, S.A. Al-Ghani, Assessment of sulfurous springs in the west of Iraq for balneotherapy, drinking, irrigation and aquaculture purposes, Environ. Geochem. Health, 36 (2014) 359–373.
[20] A.H. Kamel, S.O. Sulaiman, A.S. Mustaffa, Study of the effects of water level depression in Euphrates River on the water quality, J. Civ. Eng. Archit., 7 (2013) 238–247.
[21] M. Elhag, J.A. Bahrawi, Conservational use of remote sensing techniques for a novel rainwater harvesting in arid environment, Environ. Earth Sci., 72 (2014) 4995–5005.
[22] M. Elhag, I. Gitas, A. Othman, J. Bahrawi, P. Gikas, Assessment of water quality parameters using temporal remote sensing spectral reflectance in arid environments, Saudi Arabia, Water, 11 (2019) 556, doi: 10.3390/w11030556.
[23] J. Bahrawi, H. Ewea, A.S. Kamis, M. Elhag, Potential flood risk due to urbanization expansion in arid environments, Saudi Arabia, Nat. Hazards, 104 (2020) 795–809.
[24] J. Budiman, J. Bahrawi, A. Hidayatulloh, M. Almazroui, M. Elhag, Volumetric quantification of flash flood using microwave data on a watershed scale in arid environments, Saudi Arabia, Sustainability, 13 (2021) 4115, doi: 10.3390/su13084115.
[25] N. Al-Ansari, Management of water resources in Iraq: perspectives and prognoses, Engineering, 5 (2013) 667–684.
[26] M. Elhag, J.A. Bahrawi, Consideration of geo-statistical analysis in soil pollution assessment caused by leachate breakout in the municipality of Thermi, Greece, Desal. Water Treat., 57 (2016) 27879–27889.
[27] M. Elhag, J.A. Bahrawi, H.K. Galal, A. Aldhebiani, A.A.M. Al-Ghamdi, Stream network pollution by olive oil wastewater risk assessment in Crete, Greece, Environ. Earth Sci., 76 (2017) 278, doi: 10.1007/s12665-017-6592-y.
[28] A. Abdel Reheem, N. Yilmaz, M. Elhag, Phenolics decontamination of olive mill wastewater using onion solid by-products homogenate, Desal. Water Treat., 159 (2019) 32–39.
[29] B.M. Hussien, A.S. Fayyadh, J.M. Hammed, M.A. Al Hamdani, Hydrochemical model and probable pollution in the water of Euphrates River (Qaem–Falluja), Arabian J. Geosci., 6 (2013) 783–799.
[30] K. Banat, Y. Al-Rawi, Hydrogeochemistry, clay minerals and carbonates of the Euphrates River Iraqi, Iraqi J. Sci., 27 (1986) 347–362.
[31] M. Aljahdali, M. Elhag, Y. Mufrreh, A. Memesh, S. AlSoubhi, I.S. Zalmout, Upper Eocene calcareous nannofossil biostratigraphy: a new preliminary Priabonian record from northern Saudi Arabia, Appl. Ecol. Environ. Res., 18 (2020) 5607–5625.
[32] S. Jassim, J. Goff, Geology of Iraq, Published by Dolin, Prague and Moravian Museum, Brno, Printed in the Czech Republic, 2006.
[33] N. Yilmaz, C.H. Yardimci, M. Elhag, C.A. Dumitrache, Phytoplankton composition and water quality of Kamil Abduş Lagoon (Tuzla Lake), Istanbul-Turkey, Water, 10 (2018) 603, doi: 10.3390/w10050603.
[34] V.K. Sissakian, S.F. Fouad, Geological map of Iraq, scale 1: 1000 000, 2012, Iraqi Bull. Geol. Mining, 11 (2015) 9–16.
[35] B.M. Hussein, Hydrogeologic conditions within Al-Anbar Governorate, J. Anbar Univ. Pure Sci. Iraq., 3 (2010) 34–41.

[36] B.M. Hussien, M.A. Gharbi, Hydrogeological conditions within Abu-Jir Fault Zone (Hit–Kubaiysa), Iraqi J. Desert Stud., 2 (2010) 1–14.
[37] A.S. Al Dulaymie, B.M. Hussien, M.A. Gharbi, H.N. Mekhlif, Balneological study based on the hydrogeochemical aspects of the sulfate springs water (Hit-Kubaiysa region), Iraq, Arabian J. Geosci., 6 (2013) 801–816.
[38] F. Gilcreas, Standard Methods for the Examination of Water and Wastewater, American Journal of Public Health and the Nations Health, 1966, pp. 387–388.
[39] N. Yilmaz, R.E. Yardimci, A.T. Haghighi, M. Elhag, A. Celebi, Water quality determination by using phytoplankton composition in sea bass (*Dicentrarchus labrax*, L., 1758) aquaculture ponds in Turkey, Desal. Water Treat., 234 (2021) 392–398.
[40] T. Brikowski, Lab Notes, Hydrogeology Outdoor Laboratory, GEOS 4430, Geosciences Dept., U. Texas-Dallas, U.S., 2011, 51 p.
[41] F.T. Caruccio, The properties of groundwater, EOS, 64 (1983) 17–18.
[42] D.K. Todd, L.W. Mays, Groundwater Hydrology, John Wiley & Sons, Hoboken, New Jersey, U.S., 2004.
[43] J.D. Hem, Study and Interpretation of the Chemical Characteristics of Natural Water, 3rd ed., US Geological Survey of Water Supply, Paper 2254, USGS, Washington, DC, 1989.
[44] S. Najib, A. Fadili, K. Mehdi, J. Riss, A. Makan, Contribution of hydrochemical and geoelectrical approaches to investigate salinization process and seawater intrusion in the coastal aquifers of Chaouia, Morocco, J. Contam. Hydrol., 198 (2017) 24–36.
[45] I.G. Littlewood, T.J. Marsh, Annual freshwater river mass loads from Great Britain, 1975–1994: estimation algorithm, database and monitoring network issues, J. Hydrol., 304 (2005) 221–237.
[46] P.J. Johnes, Uncertainties in annual riverine phosphorus load estimation: impact of load estimation methodology, sampling frequency, baseflow index and catchment population density, J. Hydrol., 332 (2007) 241–258.
[47] J.R. Mullaney, D.L. Lorenz, A.D. Arntson, Chloride in Groundwater and Surface Water in Areas Underlain by the Glacial Aquifer System, Northern United States, Vol. 5086, US Geological Survey Reston, VA, 2009.
[48] Nordstrom, D. Kirk, Aqueous environmental geochemistry, Ground Water, 35 (1997) 919–920.
[49] W. Stumm, J.J. Morgan, Aquatic Chemistry: An Introduction Emphasizing Chemical Equilibria in Natural Waters, 1970.
[50] F.M. Morel, J.G. Hering, Principles and Applications of Aquatic Chemistry, John Wiley & Sons, Hoboken, New Jersey, U.S., 1993.
[51] R.G. Wetzel, G. Likens, Limnological Analyses, Springer Science & Business Media, New York, U.S., 2000.
[52] J. Van Pagee, Natural Reaeration of Surface Water by the Wind, WL|Delft Hydraulics, Report on Literature Study R1318-II, 1978 (in Dutch).
[53] G. Delvigne, Natural Reaeration of Surface Water, WL|Delft Hydraulics, Report on Literature Study, 1980.
[54] M. Allam, Q.Y. Meng, H. Al-Aizari, M. Elhag, J. Yang, M. Sakr, Z. Wang, Geo-statistical assessment of ground water quality in Dhamar Basin, Yemen, Appl. Ecol. Environ. Res., 18 (2020) 625–644.
[55] E.B. Phelps, H. Streeter, A Study of the Pollution and Natural Purification of the Ohio River, US Department of Health, Education, & Welfare, Washington, D.C., U.S., 1958.
[56] T.D. Waite, N.J. Freeman, Mathematics of Environmental Processes, Lexington Books, Michigan, U.S., 1977.
[57] G. Kiely, Environmental Engineering, Tata McGraw-Hill Education, New York, U.S., 2007.
[58] D. Omole, E. Longe, Reaeration coefficient modeling: a case study of River Atuwara in Nigeria, Res. J. Appl. Sci. Eng. Technol., 4 (2012) 1237–237.
[59] T. Srebotnjak, G. Carr, A. de Sherbinin, C. Rickwood, A global Water Quality Index and hot-deck imputation of missing data, Ecol. Indic., 17 (2012) 108–119.